

A note on the flow through porous solids at high pressures

Shankar C. Subramanian, K.R. Rajagopal*

Department of Mechanical Engineering, Texas A&M University, College Station, TX 77843-3123, USA

Received 13 September 2005; accepted 27 February 2006

Abstract

In this study we propose an equation for the flow through a porous solid that includes the equations due to Darcy and Brinkman as special sub-cases. The model is particularly well suited for describing the flow when the range of the pressure is sufficiently large, as it takes into account the possibility that the viscosity and the drag coefficient can be functions of the pressure. We can see a marked departure in the pressure field with respect to the classical Darcy solution with a narrow *boundary layer* within which the pressure suffers most of its drop.

© 2007 Elsevier Ltd. All rights reserved.

Keywords: Incompressible fluid; Porous rigid solid; Pressure dependent drag coefficient and viscosity

1. Introduction

Most problems involving the flow of a fluid through a porous solid are studied using Darcy's equation [1] or some generalization of it. While some of these modifications are ad hoc, generalizations such as those due to Brinkman [2,3] have sound physical basis. The tremendous success of Darcy's equations has unfortunately led to its being applied outside the scope of problems for which these equations apply. While the equations are most suitable for the study of flow through a rigid or nearly rigid porous solid due to moderate pressure gradients, the equations are inapplicable when the porous solid under consideration suffers significant deformation, or if the pressures and pressure gradients are exceedingly high, or if inertial effects are important. Darcy's equations are not a separate additional law of physics, as the terminology "Darcy's law" might seem to confer on them, but merely an approximation of the balance of linear momentum for the fluid that is flowing through a porous solid, within the context of "Mixture Theory".

"Mixture Theory" or the "Theory of Interacting Continua" as it stands currently owes much of its structure to the early works of Truesdell (see [4–6]) and is built upon the seminal studies of Fick [7] and Darcy [1]. Reviews of the vast literature on mixture theory can be found in the review articles by Atkin and Craine [8], Bowen [9], Bedford and Drumheller [10], several appendices to the book by Truesdell [11], and the books by Samohyl [12], and Rajagopal and Tao [13]. The equations that bear the names of Darcy, Brinkman, Biot and others can be shown to be special approximations of the balance laws for mixtures.

Recently, Rajagopal [14] has provided a systematic development of a hierarchy of approximations for the balance of linear momentum for mixtures that include Darcy's equation as the simplest of the approximations. Darcy's equation

* Corresponding author. Tel.: +1 979 862 4552.

E-mail address: krajagopal@mengr.tamu.edu (K.R. Rajagopal).

presumes that the forces exerted by the porous solid on the fluid at the pores is directly proportional to the velocity of the fluid relative to the solid, the constant of proportionality being usually referred to as the drag coefficient. While Darcy's equation takes into account the friction at the pores, it ignores the friction within the fluid in comparison to that at the pores. Also, the drag coefficient is assumed to be independent of the pressure in the fluid. While this might be reasonable under some operating conditions, it is unacceptable if the range of pressures is very large. As is well known, the viscosity of a fluid depends on the pressure (see Bridgman [15]) and the frictional resistance at the pores would also depend on the pressure leading to the drag coefficient depending on the pressure. In general, the force exerted by the porous solid on the fluid could depend on the relative acceleration (virtual mass effect), the relative spins (Magnus effect), the relative flow histories (Basset effect), etc. (see Johnson et al. [16] for a detailed discussion of the interaction forces).

In this short note we consider the effect of the drag coefficient and the viscosity depending on the pressure in a variety of ways: linearly, polynomially and exponentially. Under these assumptions for the drag coefficient and the viscosity we solve a couple of boundary value problems that have technical relevance. First, we study uniaxial flow across a porous rigid solid slab of thickness h due to a pressure gradient. The governing equations are easily integrable and exact solutions can be obtained. Even though the problem is quite trivial from the mathematical standpoint we observe that significant departures are possible from the classical Darcy solution due to the effect of high pressure; while the pressure varies linearly within the slab for the solution for Darcy's equations, it is astonishing that 80% of the pressure drop occurs within 1% of the slab thickness (see Fig. 5) when the drag coefficient depends exponentially on the pressure. *We thus have an interesting boundary layer within which the high pressure is confined.* This will have important consequences were the solid to be deformable, as one would expect, on the basis of this study, much of the deformation to occur in a narrow region adjacent to the inlet boundary. Second, we study the radial flow through a porous rigid annular cylinder. For this problem, except for the case corresponding to Darcy's law, and a few other special cases, the governing equation cannot be integrated to yield an exact solution. The problem, in general, has to be solved numerically. Once again, we find that significant departures from Darcy's law are possible. Unlike the previous example of flow through a slab, in this instance, the inertial terms do not drop out and we can thus study the effect of inertia on the flow characteristics. Interestingly, we find that the pressure profile, while being different for the case of a fluid with pressure-dependent drag coefficient and viscosity than one with constant drag coefficient and constant viscosity, is not as markedly different as in the previous example, in that one does not see a pronounced boundary layer with regard to the pressure.

2. Governing equations

We shall consider the flow of a fluid through a rigid porous solid under high pressures and high pressure gradients. Let \mathbf{v} denote the velocity of the fluid relative to the porous solid. We shall suppose that the solid has a constant porosity and that the fluid is incompressible. Thus, we shall require that

$$\operatorname{div}(\mathbf{v}) = 0. \quad (1)$$

We shall consider the following form for the Cauchy stress (\mathbf{T}) of the fluid

$$\mathbf{T} = -p\mathbf{I} + \mu(p)\mathbf{A}_1, \quad (2)$$

where $-p\mathbf{I}$ is the reaction stress due to the constraint of incompressibility, $\mu(p)$ denotes the viscosity of the fluid (which depends on the pressure p), and \mathbf{A}_1 is given by twice the symmetric part of the velocity gradient, i.e.,

$$\mathbf{A}_1 = \left[\left(\frac{\partial \mathbf{v}}{\partial \mathbf{x}} \right) + \left(\frac{\partial \mathbf{v}}{\partial \mathbf{x}} \right)^T \right]. \quad (3)$$

We shall ignore the effect of body forces. We shall assume that the resistance provided to the flow of the fluid by the solid is proportional to \mathbf{v} . Then, an appropriate approximation of the balance of linear momentum for the fluid for the problem under consideration is given by (see Rajagopal [14]):

$$-\operatorname{grad}(p) + \mu(p)\Delta \mathbf{v} + \mathbf{A}_1(\operatorname{grad}(\mu(p))) = \alpha(p)\mathbf{v} + \rho \frac{d\mathbf{v}}{dt}, \quad (4)$$

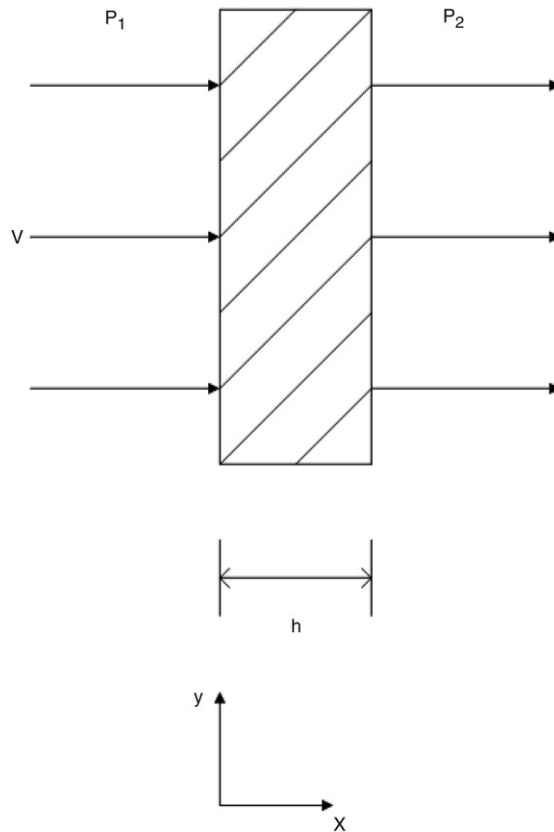


Fig. 1. Flow through a rigid porous solid slab.

where $\alpha(p)$ denotes the pressure-dependent drag coefficient, ρ is the density of the fluid, grad denotes the gradient operator, Δ denotes the Laplacian operator and $\frac{d}{dt}$ denotes the material time derivative. The viscosity $\mu(p)$ is a measure of the frictional resistance in between fluid layers while $\alpha(p)$ is a measure of the friction between the fluid and the solid, at the pore. Usually the drag coefficient α is given in terms of μ . Here, we will treat them as independent quantities. It is trivial to incorporate a dependence between $\alpha(p)$ and $\mu(p)$. In creeping flow (Stokes flow) of a Navier–Stokes fluid, Stokes [17] showed that the drag force \mathbf{F} on a sphere of radius ‘ a ’ moving with an uniform velocity \mathbf{V} is given by $\mathbf{F} = 6\pi\mu a\mathbf{V}$. The above formula holds only for creeping flow with the a priori assumption that μ is independent of the pressure. In general, α and μ are independent; α is related to the friction between the porous solid and the fluid while μ relates to the frictional effects in the fluid. The usual procedure of replacing the frictional resistance at the pores by the Stokes drag in creeping flow due to a single perfect sphere is merely a gross approximation at best. It is surprising that it works as well as it does. One usually modifies the formula for Stokes drag in an ad hoc manner to reflect flow through pores of a variety of sizes and shapes.

We note that when $\mu \equiv 0$ and α is a constant and the inertial term is ignored, Eq. (4) reduces to Darcy’s equation. If μ and α are constant and the inertial term is ignored, we have the Brinkman model and if μ is a constant and $\alpha \equiv 0$ we obtain the Navier–Stokes equation.

3. Flow across a porous rigid slab

In this section, we shall consider the flow of a fluid, whose motion is governed by Eq. (4), through a dense porous solid slab (see Fig. 1) due to a significant pressure difference. We shall assume that the slab is infinitely long along the directions of the y - and z -axes, so that the flow can be assumed to be unidirectional along the x -axis.

We shall seek a flow field of the form

$$\mathbf{v} = v(x)\mathbf{i}. \quad (5)$$

We shall further assume that the pressure field has the form

$$p = p(x). \tag{6}$$

It then follows from the constraint (1) that

$$v(x) = \text{constant} = v. \tag{7}$$

Then, Eq. (4) reduces to

$$-\frac{dp}{dx} = \alpha(p)v, \tag{8}$$

and thus the form of the viscosity μ has no effect on either the pressure or the velocity. Let us non-dimensionalize the above differential equation by setting

$$\hat{x} = \frac{x}{h}, \quad \hat{v} = \frac{v}{V}, \quad \hat{p} = \frac{p}{P_o}, \quad \hat{\alpha}(\hat{p}) = \frac{\alpha}{\alpha_o}, \tag{9}$$

where V , P_o and α_o are positive constants. Then the governing equation becomes

$$\frac{d\hat{p}}{d\hat{x}} = -\left(\frac{\alpha_o V h}{P_o}\right) \hat{\alpha}(\hat{p}) \hat{v}. \tag{10}$$

We define the non-dimensional parameter $M := \left(\frac{\alpha_o V h}{P_o}\right)$. Then, the above equation reduces to

$$\frac{d\hat{p}}{d\hat{x}} = -M \hat{\alpha}(\hat{p}) \hat{v}. \tag{11}$$

We will solve this equation along with the boundary conditions $\hat{p}(0) = \frac{p_1}{P_o} := \hat{p}_1$ and $\hat{p}(1) = \frac{p_2}{P_o} := \hat{p}_2$.

Now let us consider cases where $\hat{\alpha}(\hat{p})$ depends on the non-dimensional pressure in a variety of ways: linearly, polynomially and exponentially. For convenience, let us drop the hats atop the various quantities.

3.1. Case 1

Let us first consider the case when the drag coefficient varies exponentially with pressure, i.e.,

$$\alpha(p) = \beta_1 e^{\delta p}, \tag{12}$$

β_1 and δ being positive constants.

In this case, we obtain the pressure and the velocity as

$$p(x) = -\frac{1}{\delta} \ln[e^{-\delta p_1} (1-x) + e^{-\delta p_2} x], \tag{13}$$

$$v = \frac{1}{M \delta \beta_1} (e^{-\delta p_2} - e^{-\delta p_1}). \tag{14}$$

3.2. Case 2

Let us next consider the case where the drag coefficient is independent of pressure, i.e.,

$$\alpha(p) = \beta_1. \tag{15}$$

This choice corresponds to the form of the drag coefficient used in the classical Darcy equation.

Then, we can solve Eq. (11) to obtain

$$p(x) = p_1(1-x) + p_2 x, \tag{16}$$

Table 1

Flow through a slab — Comparison of the non-dimensional flow rate per unit cross-sectional area of the slab, q , for various choices of the drag coefficient $\alpha(p)$ and p_1 with $\beta_1 = 1$, $M = 1$ and $p_2 = 1$

$\alpha(p)$	$q (p_1 = 100)$	$q (p_1 = 200)$	$q (p_1 = 500)$
β_1	99	199	499
$\beta_1 e^{\delta p}$, $\delta = 0.01$	62.2170	85.4715	98.3312
$\beta_1 e^{\delta p}$, $\delta = 0.05$	18.8898	19.0237	19.0246
$\beta_1(1 + \delta p)$, $\delta = 0.01$	68.3197	108.8662	178.1809
$\beta_1(1 + \delta p)$, $\delta = 0.05$	34.8594	46.9821	64.1861
$\beta_1 \left(1 + \delta p + \frac{\delta^2 p^2}{2} \right)$, $\delta = 0.01$	63.3551	91.7345	123.0549
$\beta_1 \left(1 + \delta p + \frac{\delta^2 p^2}{2} \right)$, $\delta = 0.05$	23.8346	26.8141	28.9028

and

$$v = \frac{p_1 - p_2}{M\beta_1}. \tag{17}$$

3.3. Case 3

Next, let us consider a linear relationship between the drag coefficient and the pressure, i.e.,

$$\alpha(p) = \beta_1 + \beta_2 p, \tag{18}$$

where $\beta_2 := \beta_1 \delta$.

The pressure and velocity for this choice are obtained as

$$p(x) = \frac{1}{\beta_2} [(\beta_1 + \beta_2 p_1)^{(1-x)} (\beta_1 + \beta_2 p_2)^x - \beta_1], \tag{19}$$

$$v = \frac{1}{M\beta_2} \ln \left(\frac{\beta_1 + \beta_2 p_1}{\beta_1 + \beta_2 p_2} \right). \tag{20}$$

3.4. Case 4

Finally, we consider a quadratic relationship between the drag coefficient and the pressure, namely

$$\alpha(p) = \beta_1 + \beta_2 p + \beta_3 p^2, \tag{21}$$

where $\beta_3 := \frac{\beta_1 \delta^2}{2}$. Then, the solutions for p and v are found to be

$$p(x) = \frac{1}{\delta} [\tan((1-x) \tan^{-1}(\delta p_1 + 1)) + (x) \tan^{-1}(\delta p_2 + 1) - 1], \tag{22}$$

$$v = \frac{2}{M\beta_2} [\tan^{-1}(\delta p_1 + 1) - \tan^{-1}(\delta p_2 + 1)]. \tag{23}$$

We note that the flow rate per unit cross-sectional area of the slab (denoted by q) is equal to the magnitude of the velocity (v). Let us now compare the above solutions for various choices of parameter. We shall determine the velocity and pressure fields for all the above forms for $\alpha(p)$ when $\beta_1 = 1$, $\delta = 0.01$ and 0.05 , $M = 1$ and 100 , $p_2 = 1$ and $p_1 = 2, 100, 200$ and 500 . We note that the variation of the parameter M does not affect the pressure profile in all the above cases but it does affect the magnitude of the velocity. We consider only those cases where $\alpha(p)$ is a non-decreasing function of pressure. The results are presented in Tables 1 and 2. Plots of the pressure for the various cases are provided from Fig. 2 to Fig. 5. We find from Fig. 2 that when the pressure differential ($p_1 - p_2$) is small,

Table 2

Flow through a slab — Comparison of the non-dimensional flow rate per unit cross-sectional area of the slab, q , for various choices of the drag coefficient ($\alpha(p)$) and p_1 with $\beta_1 = 1$, $M = 100$ and $p_2 = 1$

$\alpha(p)$	$q (p_1 = 100)$	$q (p_1 = 200)$	$q (p_1 = 500)$
β_1	0.99	1.99	4.99
$\beta_1 e^{\delta p}$, $\delta = 0.01$	0.6221	0.8547	0.9833
$\beta_1 e^{\delta p}$, $\delta = 0.05$	0.1888	0.1902	0.1902
$\beta_1 (1 + \delta p)$, $\delta = 0.01$	0.6831	1.0886	1.7818
$\beta_1 (1 + \delta p)$, $\delta = 0.05$	0.3485	0.4698	0.6418
$\beta_1 \left(1 + \delta p + \frac{\delta^2 p^2}{2}\right)$, $\delta = 0.01$	0.6335	0.9173	1.2305
$\beta_1 \left(1 + \delta p + \frac{\delta^2 p^2}{2}\right)$, $\delta = 0.05$	0.2383	0.2681	0.2890

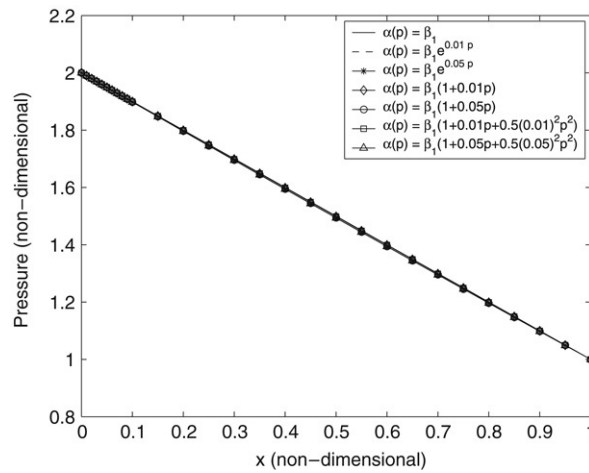


Fig. 2. Flow through a slab — Comparison of the pressure for various choices of $\alpha(p)$ with $\beta_1 = 1$, $p_1 = 2$ and $p_2 = 1$.

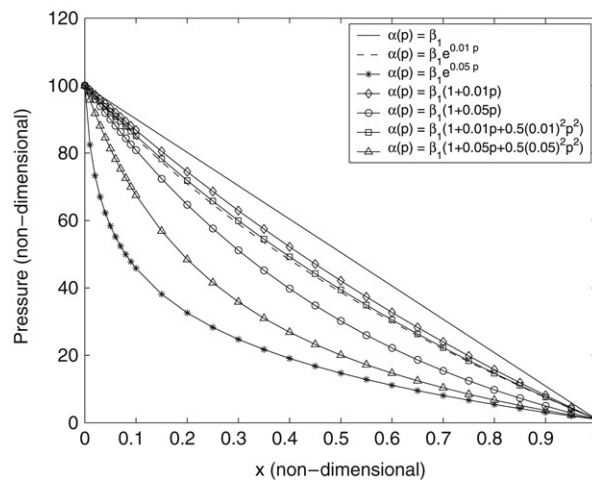


Fig. 3. Flow through a slab — Comparison of the pressure for various choices of $\alpha(p)$ with $\beta_1 = 1$, $p_1 = 100$ and $p_2 = 1$.

Darcy’s law approximates the flow quite well as long as the dependence of the drag coefficient on the pressure is mild. However, when the pressure differential is significant, we see a marked difference from the Darcy solution (see Figs. 3–5).

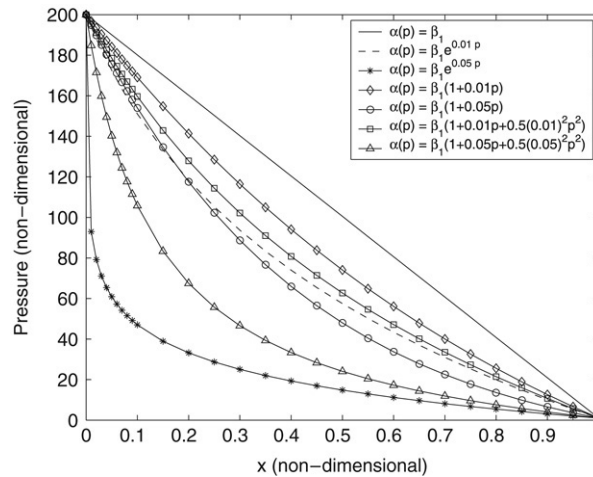


Fig. 4. Flow through a slab — Comparison of the pressure for various choices of $\alpha(p)$ with $\beta_1 = 1$, $p_1 = 200$ and $p_2 = 1$.

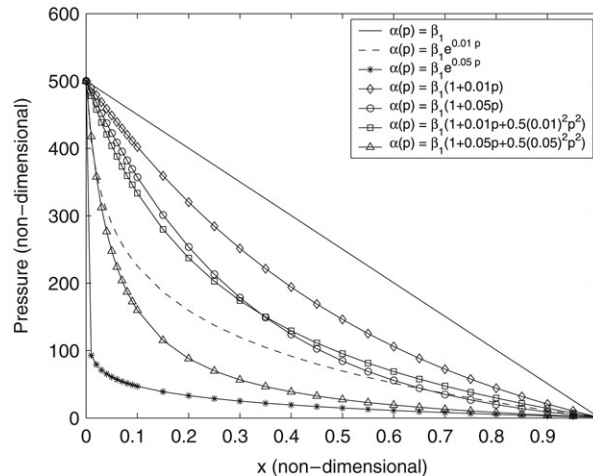


Fig. 5. Flow through a slab — Comparison of the pressure for various choices of $\alpha(p)$ with $\beta_1 = 1$, $p_1 = 500$ and $p_2 = 1$.

As is to be expected, we note from Table 1 that, for a particular pressure differential ($p_1 - p_2$), the flow rate is lower when the drag coefficient increases with pressure as opposed to the case when the drag coefficient is constant. Also, in keeping with physics, we note that, for a particular choice of δ , the flow rate is the least when the drag coefficient increases exponentially with the pressure. *What is most interesting is the tremendous decrease in the pressure within a very short distance, i.e., the development of a “pressure” boundary layer, when there is a significant pressure difference between the inlet and the outlet.* Thus, for instance, we see a pressure drop of around 70% within 5% of the slab thickness in Fig. 4 and a 80% drop in the pressure within a 1% of the thickness of the slab in Fig. 5 when the drag coefficient varies exponentially with the pressure. But this is not the case in Fig. 2, where the pressure differential ($p_1 - p_2$) is small when compared to the other cases. Here, the pressure profiles for all choices of drag coefficient are very similar to that corresponding to a constant drag coefficient, i.e., there are no significant departures from the predictions of Darcy’s equation at low pressure differentials. We note that in the case of a constant drag coefficient the flow rate increases tremendously (when compared to all the other choices of $\alpha(p)$) as the value of ($p_1 - p_2$) is increased. We find that when the drag coefficient increases with pressure, increasing the pressure differential ($p_1 - p_2$) results in a much lower increase in the flow rate when compared with the case of a constant drag coefficient.

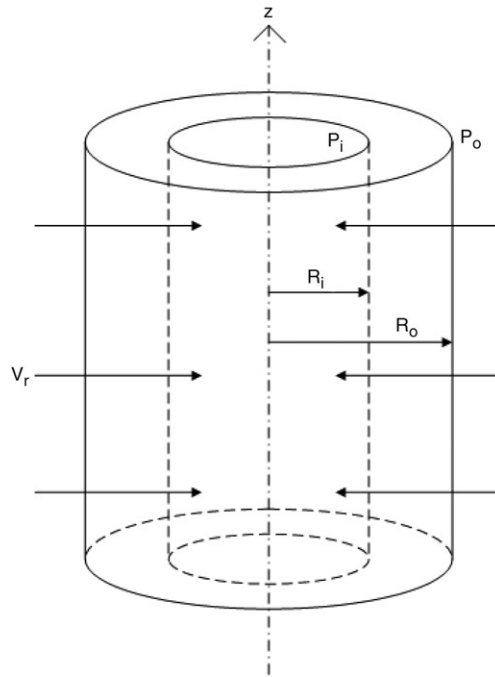


Fig. 6. Flow through a porous annular cylinder.

4. Radial flow through a porous annular cylinder

We shall now study the flow of a fluid through a dense porous solid with an annular cylindrical geometry (see Fig. 6). We assume that the cylinder is infinitely long and we consider the case when the fluid flows radially into the cylinder. We shall seek a velocity field of the form

$$\mathbf{v} = v_r(r)\mathbf{e}_r, \tag{24}$$

in a cylindrical coordinate system, where \mathbf{e}_r denotes the unit vector along the radial direction. We shall further assume that the pressure field has the form

$$p = p(r). \tag{25}$$

It follows from the constraint of incompressibility (1) that

$$\frac{dv_r(r)}{dr} + \frac{v_r}{r} = 0, \tag{26}$$

which immediately implies that

$$v_r = \frac{C}{r}, \tag{27}$$

where C is a negative constant.

We note that the flow rate into the cylinder per unit height of the same, denoted by q , is given by

$$q = -2\pi C. \tag{28}$$

Now, Eq. (4) can be reduced to

$$\left[r^2 + 2C \frac{d\mu}{dp} \right] \frac{dp}{dr} = -Cr\alpha(p) + \frac{\rho C^2}{r}. \tag{29}$$

Let us non-dimensionalize the above equations by setting

$$\hat{r} = \frac{r}{R}, \quad \hat{p} = \frac{p}{P_o}, \quad \hat{C} = \frac{C}{C_o}, \quad \hat{\mu}(\hat{p}) = \frac{\mu(p)}{\mu_o}, \quad \hat{\alpha}(\hat{p}) = \frac{\alpha(p)}{\alpha_o}, \quad \hat{v}_r = \frac{v_r}{V_o}, \quad \hat{q} = \frac{q}{q_o}, \quad (30)$$

where $R, P_o, C_o, \mu_o, \alpha_o, V_o$ and q_o are positive constants.

Then, Eqs. (27)–(29) become

$$\hat{v}_r = \left(\frac{C_o}{V_o R} \right) \frac{\hat{C}}{\hat{r}}, \quad (31)$$

$$\hat{q} = - \left(\frac{2\pi C_o}{q_o} \right) \hat{C}, \quad (32)$$

and

$$\left[\hat{r}^2 + 2 \left(\frac{C_o \mu_o}{P_o R^2} \right) \hat{C} \frac{d\hat{\mu}(\hat{p})}{d\hat{p}} \right] \frac{d\hat{p}}{d\hat{r}} = - \left(\frac{\alpha_o C_o}{P_o} \right) \hat{C} \hat{\alpha}(\hat{p}) \hat{r} + \left(\frac{\rho C_o^2}{P_o R^2} \right) \frac{\hat{C}^2}{\hat{r}}. \quad (33)$$

Let us define the following non-dimensional parameters: $N_1 = \frac{C_o \mu_o}{P_o R^2}$, $N_2 = \frac{\alpha_o C_o}{P_o}$ and $N_3 = \frac{\rho C_o^2}{P_o R^2}$. We note that N_1 , N_2 and N_3 are positive. Then, the above equation reduces to

$$\left[\hat{r}^2 + 2N_1 \hat{C} \frac{d\hat{\mu}(\hat{p})}{d\hat{p}} \right] \frac{d\hat{p}}{d\hat{r}} = -N_2 \hat{C} \hat{\alpha}(\hat{p}) \hat{r} + \frac{N_3 \hat{C}^2}{\hat{r}}. \quad (34)$$

We integrate the above equation to obtain the pressure for various choices of $\hat{\mu}(\hat{p})$ and $\hat{\alpha}(\hat{p})$ along with the boundary conditions $\hat{p}(\hat{r} = (R_i/R) := \hat{R}_i) = p_i/P_o := \hat{p}_i$ and $\hat{p}(\hat{r} = (R_o/R) := \hat{R}_o) = p_o/P_o := \hat{p}_o$. Here, R_i and R_o denote the inner and outer radius of the annular cylinder respectively with p_i and p_o being the pressure at the inner and the outer surface of the annular cylinder respectively. We note from Eq. (32) that a comparison of \hat{C} for various choices of the drag coefficient and the viscosity is equivalent to a comparison of the flow rate per unit height of the cylinder. For convenience, we will drop the hats atop the various quantities. Thus, Eq. (34) can be rewritten as

$$\left[r^2 + 2N_1 C \frac{d\mu(p)}{dp} \right] \frac{dp}{dr} = -N_2 C \alpha(p) r + \frac{N_3 C^2}{r}. \quad (35)$$

We will consider only those cases where $\mu(p)$ and $\alpha(p)$ are non-decreasing functions of p . Hence the term $\frac{d\mu(p)}{dp}$ will be non-negative. We note that the right-hand side of the above equation is positive at all points in the domain of interest. For the problem under consideration, $\frac{dp}{dr}$ is also positive. Hence, the various parameters have to be chosen in such a way that the term $\left[r^2 + 2N_1 C \frac{d\mu(p)}{dp} \right]$ is positive. In general, we solve the differential equation numerically to obtain p and C , and we provide exact solutions when possible. The procedure used in solving the equation numerically is as follows. We initially take the parameter C to be zero and solve Eq. (35) using the fourth-order Runge–Kutta method along with the condition that $p(R_i) = p_i$. Then, the value of the pressure at the outer surface is evaluated and compared with the value of p_o that has been prescribed. The value of C is decreased at the end of each iteration until the absolute value of the difference between $p(R_o)$ and p_o becomes less than or equal to 10^{-3} . We shall set the value of the parameter N_3 to be zero in the instances where we neglect the inertial term. We compare the results between the various cases for the following choice of parameters:

$$\begin{aligned} R_i &= 1, & R_o &= 10, & N_1 &= 0.5, & N_2 &= 1, & p_i &= 1, & \beta_1 &= 1, & A_1 &= 1, \\ V_o &= \frac{C_o}{R}, & q_o &= 2\pi C_o. \end{aligned} \quad (36)$$

We shall compare the solutions corresponding to two values of p_o : 100 and 200; and two values of N_3 : 0 and 0.1.

4.1. $\mu(p) = A_1$, where A_1 is a positive constant

We calculate the constant C in each case and tabulate the values obtained.

(1) $\alpha(p) = \beta_1$. The governing equation (35) reduces to

$$r^2 \frac{dp}{dr} = -N_2 C \beta_1 r + \frac{N_3 C^2}{r}. \tag{37}$$

This equation can be integrated to obtain

$$p(r) = -N_2 \beta_1 C \ln(r) - \frac{N_3 C^2}{2r^2} + D, \tag{38}$$

where D is the constant of integration. When $N_3 = 0$, i.e., when we neglect the inertial term, we obtain

$$p(r) = \frac{1}{\ln\left(\frac{R_o}{R_i}\right)} \left[p_o \ln\left(\frac{r}{R_i}\right) + p_i \ln\left(\frac{R_o}{r}\right) \right], \tag{39}$$

$$C = \frac{(p_i - p_o)}{N_2 \beta_1 \ln\left(\frac{R_o}{R_i}\right)}. \tag{40}$$

(2) $\alpha(p) = \beta_1 e^{\delta p}$. The governing equation becomes

$$r^2 \frac{dp}{dr} = -N_2 C \beta_1 e^{\delta p} r + \frac{N_3 C^2}{r}. \tag{41}$$

When $N_3 = 0$, this equation can be solved to obtain

$$p(r) = -\frac{1}{\delta} \ln \left(\frac{1}{\ln\left(\frac{R_o}{R_i}\right)} \left[e^{-\delta p_o} \ln\left(\frac{r}{R_i}\right) + e^{-\delta p_i} \ln\left(\frac{R_o}{r}\right) \right] \right), \tag{42}$$

$$C = \frac{e^{-\delta p_o} - e^{-\delta p_i}}{N_2 \beta_1 \delta \ln\left(\frac{R_o}{R_i}\right)}. \tag{43}$$

(3) $\alpha(p) = \beta_1 + \beta_2 p$. The governing equation for this choice is

$$r^2 \frac{dp}{dr} = -N_2 C r (\beta_1 + \beta_2 p) + \frac{N_3 C^2}{r}. \tag{44}$$

When $N_3 = 0$, the solution to this equation is

$$p(r) = \frac{1}{\beta_2} \left(\exp \left[\frac{1}{\ln\left(\frac{R_o}{R_i}\right)} \left(\ln(\beta_1 + \beta_2 p_o) \ln\left(\frac{r}{R_i}\right) + \ln(\beta_1 + \beta_2 p_i) \ln\left(\frac{R_o}{r}\right) \right) \right] - \beta_1 \right), \tag{45}$$

$$C = \frac{1}{N_2 \beta_2 \ln\left(\frac{R_o}{R_i}\right)} \ln \left(\frac{\beta_1 + \beta_2 p_i}{\beta_1 + \beta_2 p_o} \right). \tag{46}$$

(4) $\alpha(p) = \beta_1 + \beta_2 p + \beta_3 p^2$. The governing equation in this case is

$$r^2 \frac{dp}{dr} = -N_2 C r (\beta_1 + \beta_2 p + \beta_3 p^2) + \frac{N_3 C^2}{r}. \tag{47}$$

When $N_3 = 0$, the solution is

$$p(r) = \frac{1}{\delta} \left[\tan \left(\frac{1}{\ln\left(\frac{R_o}{R_i}\right)} \left[\tan^{-1}(\delta p_o + 1) \ln\left(\frac{r}{R_i}\right) + \tan^{-1}(\delta p_i + 1) \ln\left(\frac{R_o}{r}\right) \right] \right) - 1 \right], \tag{48}$$

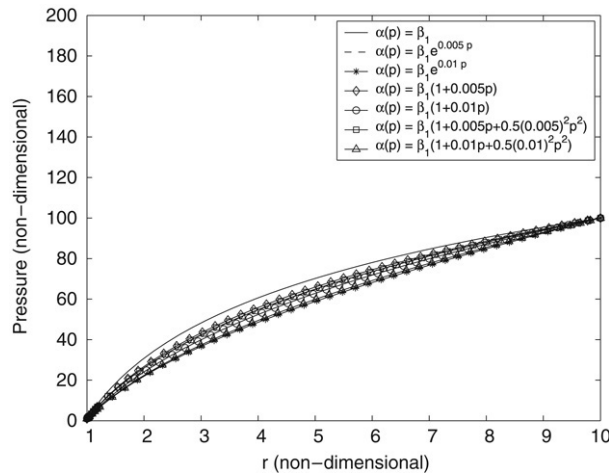


Fig. 7. Flow through an annular cylinder — Plot of pressure for $\mu(p) = A_1$, $p_i = 1$, $p_o = 100$, $N_2 = 1$ and $N_3 = 0$.

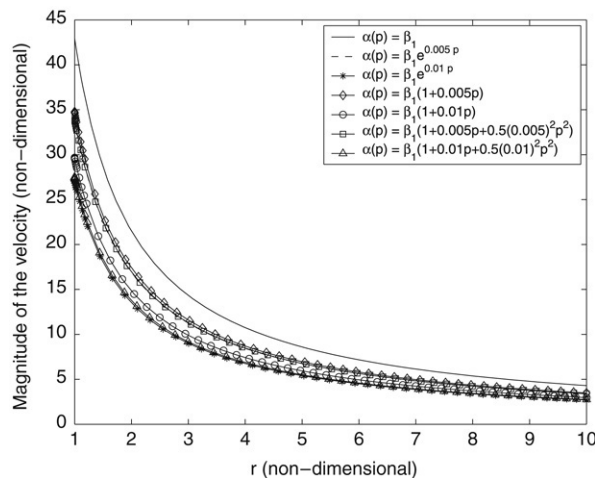


Fig. 8. Flow through an annular cylinder — Plot of velocity for $\mu(p) = A_1$, $p_i = 1$, $p_o = 100$, $N_2 = 1$ and $N_3 = 0$.

$$C = \frac{2}{N_2 \beta_2 \ln\left(\frac{R_o}{R_i}\right)} \left[\tan^{-1}(\delta p_i + 1) - \tan^{-1}(\delta p_o + 1) \right]. \tag{49}$$

In Table 3, we compare the flow rate (q) obtained for the above cases. Representative plots of the pressure and velocity for one of these cases are provided in Figs. 7 and 8 respectively. We note that the flow rate decreases as the drag coefficient increases with pressure. We also note that the inclusion of the inertial term results in a decrease in the flow rate. As is to be expected, the flow rate increases with an increase in the pressure differential ($p_o - p_i$).

4.2. $\mu(p) = A_1 e^{\gamma p}$, $\gamma > 0$

(1) $\alpha(p) = \beta_1$. In this case, the governing equation (35) becomes

$$(r^2 + 2\gamma N_1 A_1 C e^{\gamma p}) \frac{dp}{dr} = -N_2 C \beta_1 r + \frac{N_3 C^2}{r}. \tag{50}$$

When $N_3 = 0$, the solution to this equation is

$$N_2 C \beta_1 \exp\left(\frac{2p}{N_2 C \beta_1}\right) \left[\frac{r^2}{2} + \frac{2N_1 A_1 \gamma C}{(2 + N_2 C \beta_1 \gamma)} e^{\gamma p} \right] = D. \tag{51}$$

Table 3

Flow through an annular cylinder — Comparison of the non-dimensional flow rate (q) for $\mu(p) = A_1$, $N_2 = 1$, $p_i = 1$, $A_1 = 1$ and $\beta_1 = 1$

$\alpha(p)$	$N_3 = 0$		$N_3 = 0.1$	
	$q(p_o = 100)$	$q(p_o = 200)$	$q(p_o = 100)$	$q(p_o = 200)$
β_1	42.9947	86.4239	27.1490	44.2771
$\beta_1 e^{\delta p}$, $\delta = 0.005$	33.7428	54.4719	23.4130	34.4347
$\beta_1 e^{\delta p}$, $\delta = 0.01$	27.0203	37.1197	20.0482	26.3406
$\beta_1(1 + \delta p)$, $\delta = 0.005$	34.7847	59.7725	23.9184	36.6794
$\beta_1(1 + \delta p)$, $\delta = 0.01$	29.6706	47.2798	21.5353	31.7716
$\beta_1 \left(1 + \delta p + \frac{\delta^2 p^2}{2}\right)$, $\delta = 0.005$	33.8576	55.4604	23.4716	34.8910
$\beta_1 \left(1 + \delta p + \frac{\delta^2 p^2}{2}\right)$, $\delta = 0.01$	27.5145	39.8397	20.3413	27.9242

Table 4

Flow through an annular cylinder — Comparison of the non-dimensional flow rate (q) for $\mu(p) = A_1 e^{\gamma p}$, $\gamma = 0.005$, $N_1 = 0.5$, $N_2 = 1$, $p_i = 1$, $A_1 = 1$ and $\beta_1 = 1$

$\alpha(p)$	$N_3 = 0$		$N_3 = 0.1$	
	$q(p_o = 100)$	$q(p_o = 200)$	$q(p_o = 100)$	$q(p_o = 200)$
β_1	40.7392	76.0811	26.1548	41.1388
$\beta_1 e^{\delta p}$, $\delta = 0.005$	32.3789	50.6323	22.6987	32.7145
$\beta_1 e^{\delta p}$, $\delta = 0.01$	26.1591	35.4190	19.5397	25.4087
$\beta_1(1 + \delta p)$, $\delta = 0.005$	33.3313	55.0748	23.1695	34.6808
$\beta_1(1 + \delta p)$, $\delta = 0.01$	28.6239	44.4179	20.9409	30.3393
$\beta_1 \left(1 + \delta p + \frac{\delta^2 p^2}{2}\right)$, $\delta = 0.005$	32.4840	51.4668	22.7533	33.1163
$\beta_1 \left(1 + \delta p + \frac{\delta^2 p^2}{2}\right)$, $\delta = 0.01$	26.6201	37.8583	19.8166	26.8600

(2) $\alpha(p) = \beta_1 e^{\delta p}$. The governing equation in this case reduces to

$$(r^2 + 2\gamma N_1 A_1 C e^{\gamma p}) \frac{dp}{dr} = -N_2 C \beta_1 r e^{\delta p} + \frac{N_3 C^2}{r}. \tag{52}$$

(3) $\alpha(p) = \beta_1 + \beta_2 p$. The governing equation now becomes

$$(r^2 + 2\gamma N_1 A_1 C e^{\gamma p}) \frac{dp}{dr} = -N_2 C r (\beta_1 + \beta_2 p) + \frac{N_3 C^2}{r}. \tag{53}$$

(4) $\alpha(p) = \beta_1 + \beta_2 p + \beta_3 p^2$. The governing equation for this case is

$$(r^2 + 2\gamma N_1 A_1 C e^{\gamma p}) \frac{dp}{dr} = -N_2 C r (\beta_1 + \beta_2 p + \beta_3 p^2) + \frac{N_3 C^2}{r}. \tag{54}$$

In Tables 4 and 5, we compare the flow rate obtained for the various cases considered in this subsection for $\gamma = 0.005$ and $\gamma = 0.01$ respectively. The pressure and velocity vary in a manner that is qualitatively similar to that depicted in Figs. 7 and 8. Once again we find a decrease in the flow rate as the viscosity increases with pressure.

4.3. $\mu(p) = A_1 + A_2 p$, $A_2 := A_1 \gamma$

(1) $\alpha(p) = \beta_1$. The governing equation now reduces to

$$(r^2 + 2N_1 A_2 C) \frac{dp}{dr} = -N_2 C \beta_1 r + \frac{N_3 C^2}{r}. \tag{55}$$

When we neglect inertial effects, this equation can be solved to yield

$$p(r) = -\frac{N_2 \beta_1 C}{2} \ln(r^2 + 2N_1 A_2 C) + D. \tag{56}$$

Table 5

Flow through an annular cylinder — Comparison of the non-dimensional flow rate (q) for $\mu(p) = A_1 e^{\gamma p}$, $\gamma = 0.01$, $N_1 = 0.5$, $N_2 = 1$, $p_i = 1$, $A_1 = 1$ and $\beta_1 = 1$

$\alpha(p)$	$N_3 = 0$		$N_3 = 0.1$	
	$q (p_o = 100)$	$q (p_o = 200)$	$q (p_o = 100)$	$q (p_o = 200)$
β_1	37.8552	60.3209	24.8557	35.8518
$\beta_1 e^{\delta p}$, $\delta = 0.005$	30.6908	45.1623	21.7943	30.0780
$\beta_1 e^{\delta p}$, $\delta = 0.01$	25.1226	33.1705	18.9154	24.1169
$\beta_1(1 + \delta p)$, $\delta = 0.005$	31.5232	48.2280	22.2159	31.5232
$\beta_1(1 + \delta p)$, $\delta = 0.01$	27.3455	40.3873	20.1986	28.1782
$\beta_1 \left(1 + \delta p + \frac{\delta^2 p^2}{2}\right)$, $\delta = 0.005$	30.7827	45.7481	21.8432	30.3768
$\beta_1 \left(1 + \delta p + \frac{\delta^2 p^2}{2}\right)$, $\delta = 0.01$	25.5402	35.1827	19.1698	25.3415

(2) $\alpha(p) = \beta_1 e^{\delta p}$. The governing equation becomes

$$(r^2 + 2N_1 A_2 C) \frac{dp}{dr} = -N_2 C \beta_1 r e^{\delta p} + \frac{N_3 C^2}{r}. \tag{57}$$

When $N_3 = 0$, the solution to this equation is

$$p(r) = -\frac{1}{\delta} \ln \left[\frac{N_2 C \beta_1 \delta}{2} \ln(r^2 + 2N_1 A_2 C) + D \right]. \tag{58}$$

(3) $\alpha(p) = \beta_1 + \beta_2 p$. The governing equation for this choice is

$$(r^2 + 2N_1 A_2 C) \frac{dp}{dr} = -N_2 C r (\beta_1 + \beta_2 p) + \frac{N_3 C^2}{r}. \tag{59}$$

On neglecting the inertia term, the solution to this equation is

$$p(r) = \frac{1}{\beta_2} \left[D (r^2 + 2N_1 A_2 C)^{-\frac{N_2 C \beta_2}{2}} - \beta_1 \right]. \tag{60}$$

(4) $\alpha(p) = \beta_1 + \beta_2 p + \beta_3 p^2$. The governing equation in this case is

$$(r^2 + 2N_1 A_2 C) \frac{dp}{dr} = -N_2 C r (\beta_1 + \beta_2 p + \beta_3 p^2) + \frac{N_3 C^2}{r}. \tag{61}$$

When $N_3 = 0$, the solution to this equation is

$$p(r) = \frac{\beta_2}{2\beta_3} \left[\tan \left(-\frac{N_2 C \beta_1 \delta}{4} \ln(r^2 + 2N_1 A_2 C) + D \right) - 1 \right]. \tag{62}$$

In Tables 6 and 7, we compare the flow rate obtained for the above choices of $\alpha(p)$ with $\gamma = 0.005$ and $\gamma = 0.01$ respectively. The pressure and velocity for one of these cases are plotted in Figs. 9 and 10.

4.4. $\mu(p) = A_1 + A_2 p + A_3 p^2$, $A_3 := \frac{A_1 \gamma^2}{2}$

(1) $\alpha(p) = \beta_1$. The governing equation becomes

$$(r^2 + 2N_1 A_2 C + 4N_1 A_3 C p) \frac{dp}{dr} = -N_2 C \beta_1 r + \frac{N_3 C^2}{r}. \tag{63}$$

If we neglect the inertial term, the solution to this equation is

$$\left(\frac{N_2 C \beta_1}{2} \right) \exp \left(\frac{2p}{N_2 C \beta_1} \right) [r^2 + 2N_1 A_2 C + 4N_1 A_3 C p - 2N_1 N_2 A_3 \beta_1 C^2] = D. \tag{64}$$

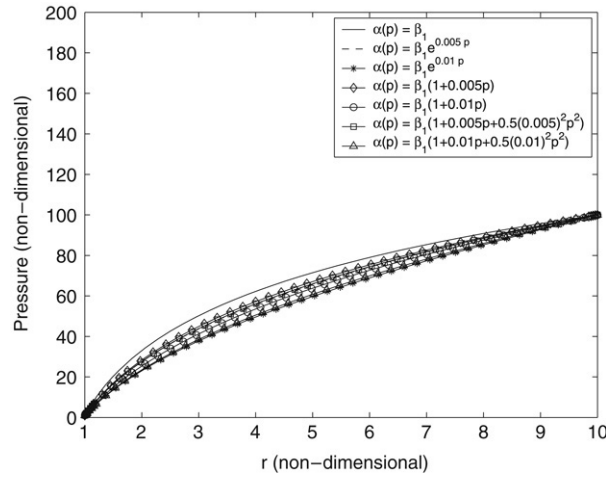


Fig. 9. Flow through an annular cylinder — Plot of pressure for $\mu(p) = A_1 + A_2p$, $\gamma = 0.005$, $p_i = 1$, $p_o = 100$, $N_1 = 0.5$, $N_2 = 1$ and $N_3 = 0$.

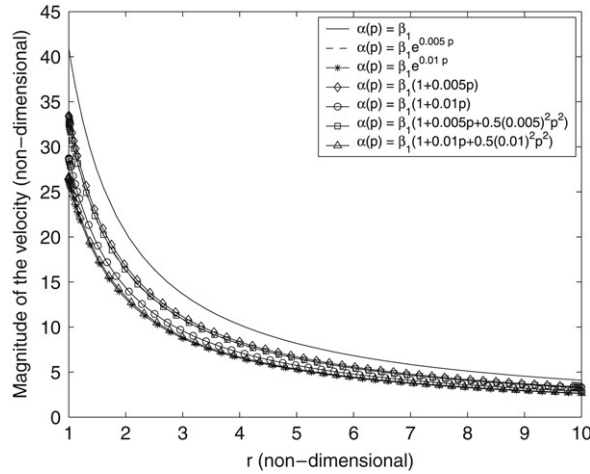


Fig. 10. Flow through an annular cylinder — Plot of velocity for $\mu(p) = A_1 + A_2p$, $\gamma = 0.005$, $p_i = 1$, $p_o = 100$, $N_1 = 0.5$, $N_2 = 1$ and $N_3 = 0$.

Table 6

Flow through an annular cylinder — Comparison of the non-dimensional flow rate (q) for $\mu(p) = A_1 + A_2p$, $\gamma = 0.005$, $N_1 = 0.5$, $N_2 = 1$, $p_i = 1$, $A_1 = 1$ and $\beta_1 = 1$

$\alpha(p)$	$N_3 = 0$		$N_3 = 0.1$	
	$q (p_o = 100)$	$q (p_o = 200)$	$q (p_o = 100)$	$q (p_o = 200)$
β_1	40.9731	78.0944	26.2755	41.9015
$\beta_1 e^{\delta p}$, $\delta = 0.005$	32.5025	51.2109	22.7747	33.0422
$\beta_1 e^{\delta p}$, $\delta = 0.01$	26.2272	35.6166	19.5865	25.5418
$\beta_1(1 + \delta p)$, $\delta = 0.005$	33.4660	55.8368	23.2510	35.0914
$\beta_1(1 + \delta p)$, $\delta = 0.01$	28.7132	44.8307	21.0003	30.5991
$\beta_1 \left(1 + \delta p + \frac{\delta^2 p^2}{2}\right)$, $\delta = 0.005$	32.6088	52.0785	22.8300	33.4604
$\beta_1 \left(1 + \delta p + \frac{\delta^2 p^2}{2}\right)$, $\delta = 0.01$	26.6920	38.1062	19.8658	27.0253

Table 7

Flow through an annular cylinder — Comparison of the non-dimensional flow rate (q) for $\mu(p) = A_1 + A_2p$, $\gamma = 0.01$, $N_1 = 0.5$, $N_2 = 1$, $p_i = 1$, $A_1 = 1$ and $\beta_1 = 1$

$\alpha(p)$	$N_3 = 0$		$N_3 = 0.1$	
	$q(p_o = 100)$	$q(p_o = 200)$	$q(p_o = 100)$	$q(p_o = 200)$
β_1	38.8725	68.9877	25.3879	39.4684
$\beta_1 e^{\delta p}$, $\delta = 0.005$	31.2255	47.7802	22.1270	31.6197
$\beta_1 e^{\delta p}$, $\delta = 0.01$	25.4159	34.0640	19.1188	24.7291
$\beta_1(1 + \delta p)$, $\delta = 0.005$	32.1071	51.6713	22.5737	33.4674
$\beta_1(1 + \delta p)$, $\delta = 0.01$	27.7314	42.2744	20.4578	29.4022
$\beta_1 \left(1 + \delta p + \frac{\delta^2 p^2}{2}\right)$, $\delta = 0.005$	31.3229	48.5167	22.1789	31.9986
$\beta_1 \left(1 + \delta p + \frac{\delta^2 p^2}{2}\right)$, $\delta = 0.01$	25.8501	36.3108	19.3839	26.1100

Table 8

Flow through an annular cylinder — Comparison of the non-dimensional flow rate (q) for $\mu(p) = A_1 + A_2p + A_3p^2$, $\gamma = 0.005$, $N_1 = 0.5$, $N_2 = 1$, $p_i = 1$, $A_1 = 1$ and $\beta_1 = 1$

$\alpha(p)$	$N_3 = 0$		$N_3 = 0.1$	
	$q(p_o = 100)$	$q(p_o = 200)$	$q(p_o = 100)$	$q(p_o = 200)$
β_1	40.7606	76.4269	26.1665	41.2863
$\beta_1 e^{\delta p}$, $\delta = 0.005$	32.3894	50.7196	22.7055	32.7678
$\beta_1 e^{\delta p}$, $\delta = 0.01$	26.1644	35.4445	19.5435	25.4264
$\beta_1(1 + \delta p)$, $\delta = 0.005$	33.3429	55.1958	23.1768	34.7516
$\beta_1(1 + \delta p)$, $\delta = 0.01$	28.6313	44.4804	20.9460	30.3809
$\beta_1 \left(1 + \delta p + \frac{\delta^2 p^2}{2}\right)$, $\delta = 0.005$	32.4946	51.5603	22.7602	33.1731
$\beta_1 \left(1 + \delta p + \frac{\delta^2 p^2}{2}\right)$, $\delta = 0.01$	26.6257	37.8925	19.8206	26.8837

(2) $\alpha(p) = \beta_1 e^{\delta p}$. The governing equation reduces to

$$(r^2 + 2N_1 A_2 C + 4N_1 A_3 C p) \frac{dp}{dr} = -N_2 C \beta_1 r e^{\delta p} + \frac{N_3 C^2}{r}. \tag{65}$$

(3) $\alpha(p) = \beta_1 + \beta_2 p$. The governing equation in this case is

$$(r^2 + 2N_1 A_2 C + 4N_1 A_3 C p) \frac{dp}{dr} = -N_2 C r (\beta_1 + \beta_2 p) + \frac{N_3 C^2}{r}. \tag{66}$$

(4) $\alpha(p) = \beta_1 + \beta_2 p + \beta_3 p^2$. The governing equation for this choice becomes

$$(r^2 + 2N_1 A_2 C + 4N_1 A_3 C p) \frac{dp}{dr} = -N_2 C r (\beta_1 + \beta_2 p + \beta_3 p^2) + \frac{N_3 C^2}{r}. \tag{67}$$

In Tables 8 and 9, we compare the flow rate obtained for the various cases considered in this subsection with $\gamma = 0.005$ and $\gamma = 0.01$ respectively. The plots for the pressure and velocity are qualitatively similar to Figs. 9 and 10 and hence we shall not document them here.

5. Concluding remarks

In this article, we have studied the flow of a fluid through a porous rigid solid under high pressures and high pressure gradients. We have studied two boundary value problems involving the flow of the fluid through a solid porous slab and an annular cylinder. We have allowed the drag coefficient and the fluid viscosity to vary with pressure in different ways. We have observed that there is an appreciable decrease in the flow rate when the drag coefficient increases with pressure compared with the case when it is assumed to be a constant. We also find that boundary layers, in the sense

Table 9

Flow through an annular cylinder — Comparison of the non-dimensional flow rate (q) for $\mu(p) = A_1 + A_2p + A_3p^2$, $\gamma = 0.01$, $N_1 = 0.5$, $N_2 = 1$, $p_i = 1$, $A_1 = 1$ and $\beta_1 = 1$

$\alpha(p)$	$N_3 = 0$		$N_3 = 0.1$	
	$q(p_o = 100)$	$q(p_o = 200)$	$q(p_o = 100)$	$q(p_o = 200)$
β_1	38.0296	62.6617	24.9544	37.0719
$\beta_1 e^{\delta p}$, $\delta = 0.005$	30.7771	45.8681	21.8511	30.5384
$\beta_1 e^{\delta p}$, $\delta = 0.01$	25.1667	33.3883	18.9471	24.2723
$\beta_1(1 + \delta p)$, $\delta = 0.005$	31.6187	49.1853	22.2781	32.1311
$\beta_1(1 + \delta p)$, $\delta = 0.01$	27.4066	40.9085	20.2415	28.5413
$\beta_1 \left(1 + \delta p + \frac{\delta^2 p^2}{2}\right)$, $\delta = 0.005$	30.8700	46.5015	21.9007	30.8669
$\beta_1 \left(1 + \delta p + \frac{\delta^2 p^2}{2}\right)$, $\delta = 0.01$	25.5874	35.4738	19.2038	25.5497

of narrow layers wherein the pressure is large, can develop in certain geometries. As is to be expected, we found that the flow rate decreases as the viscosity and drag coefficient increase with pressure. We also found that inertia tends to decrease the flow rate. The most important finding of the study is that marked departures from the predictions of “Darcy’s law” are possible when the viscosity and drag coefficient depend upon the pressure.

Acknowledgment

We thank the National Science Foundation for support of this work.

References

- [1] H. Darcy, *Les fontaines publiques de la ville de Dijon*, Victor Dalmont, Paris, 1856.
- [2] H.C. Brinkman, A calculation of the viscous force exerted by a flowing fluid on a dense swarm of particles, *Applied Scientific Research A1* (1947) 27–34.
- [3] H.C. Brinkman, On the permeability of media consisting of closely packed porous particles, *Applied Scientific Research A1* (1947) 81–86.
- [4] C. Truesdell, *Sulle basi della termomeccanica*, Nota I, *Rendiconti Lincei* 22 (1957) 33–38.
- [5] C. Truesdell, *Sulle basi della termomeccanica*, Nota II, *Rendiconti Lincei* 22 (1957) 158–166.
- [6] C. Truesdell, Mechanical basis of diffusion, *Journal of Chemical Physics* 37 (10) (1962) 2336–2344.
- [7] A. Fick, Ueber diffusion, *Annalen der Physik und Chemie* 94 (1855) 59–86.
- [8] R.J. Atkin, R.E. Craine, Continuum theories of mixtures: Basic theory and historical development, *Quarterly Journal of Mechanics and Applied Mathematics* 29 (1976) 209–244.
- [9] R.M. Bowen, Theory of Mixtures, in: A.C. Eringen (Ed.), *Continuum Physics*, vol. III, Academic Press, New York, 1976, pp. 1–127.
- [10] A. Bedford, D.S. Drumheller, Theories of immiscible and structured mixtures, *International Journal of Engineering Science* 21 (8) (1983) 863–960.
- [11] C. Truesdell, *Rational Thermodynamics*, second ed., Springer Verlag, New York, 1984.
- [12] I. Samohyl, *Thermodynamics of Irreversible Processes in Fluid Mixtures*, Teubner, Leipzig, 1987.
- [13] K.R. Rajagopal, L. Tao, *Mechanics of Mixtures*, World Scientific, New Jersey, 1995.
- [14] K.R. Rajagopal, On a hierarchy of approximate models for flows of incompressible fluids through porous solids, *Mathematical Models and Methods in the Applied Sciences* 17 (2) (2007) 215–252.
- [15] P.W. Bridgman, *The Physics of High Pressure*, MacMillan, New York, 1931.
- [16] G. Johnson, M. Massoudi, K.R. Rajagopal, A review of interaction mechanisms in fluid–solid flows, Tech. Rep. DOE/PETC/TR-90/9, Pittsburg Energy Technology Center, Pittsburg, Pennsylvania, September 1990.
- [17] G.G. Stokes, On the effect of the internal friction of fluids on the motion of pendulums, *Transactions of the Cambridge Philosophical Society* 9 (1850) 8–106.